

bandwidth. Coupling is maximum when the patch is centred over the aperture, but small alignment errors cause little change.

The data presented are based on a linear array of 15 identical slot-patch radiating elements. A typical return loss and insertion loss measurement is shown in Fig. 2. The E- and H-plane patterns are shown in Fig. 3. The waveguide dimensions were chosen such that the main beam is scanned 35 degrees off the broadside in the E-plane. The H-plane pattern is measured in a conical-scan manner through the beam maximum.

Assuming that all the radiators in the linear array have the same characteristics and that losses are negligible, the coupling factor (ratio of power in the waveguide incident on the element to the power radiated by the element) for each element of the 15 element array is related to the insertion loss,  $IL$  (dB) by

$$CF \text{ (dB)} = -10 \log \left[ 1 - 10^{-IL \text{ (dB)}/150} \right] \quad (1)$$

Several 15-element linear arrays were measured to characterise their performance (Fig. 4). The resonant frequency is controlled primarily by the patch length. The size and inclination angle of the slot control the coupling factor and slightly tune the frequency.

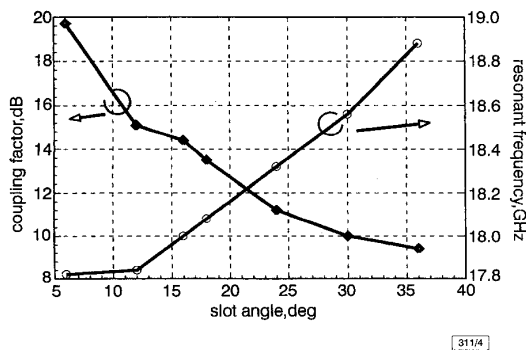


Fig. 4 Characteristics of slot-patch element

Slot size =  $0.44 \times 2.80$ mm, patch size =  $3.10 \times 4.09$ mm, substrate thickness = 0.0254mm,  $\epsilon_r = 2.2$

For coupling weaker than  $-15$ dB ( $CF > 15$ dB), the measured main beam direction of the linear array is accurately determined by the waveguide broad wall dimension  $a$ :

$$\theta = \sin^{-1} \sqrt{1 - \left( \frac{\lambda}{2a} \right)^2} \quad (2)$$

for a forward-fire beam. This suggests that the propagating  $TE_{10}$  mode inside the waveguide is not greatly perturbed by the coupling mechanism for weak-to-medium coupling factors. For these cases, the propagation constant ( $\beta_g = 2\pi/\lambda_g$ ) is independent of the coupling factor, so design of a specific amplitude distribution over the array surface requires only that the printed patches and slots are controlled. The dimensions of the waveguide channel remain constant and compensation of  $\beta_g$ , as in [5], is not needed to maintain the scan angle.

Planar arrays can be fabricated by machining several waveguide channels like that of Fig. 1b. The microstrip patches and apertures are etched on double-clad substrate. The ground plane then is soldered onto the waveguide walls to complete the antenna. Adjacent waveguide channels can be used to realise transverse polarisation by etching longitudinal slots on the ground plane side. Patches are not required for transverse polarisation and the substrate serves as a radome. This allows fabrication of both polarisations with a single piece of substrate.

Since rectangular patches are intrinsically linearly polarised radiators, the cross-polarisation introduced by the tilted slot is reduced. If a back-fire main beam is desired, slots with alternate tilt directions can be employed to further reduce the cross-polarisation.

Drawbacks for this configuration are: (i) relatively narrow bandwidth because of the high-Q nature of the patches, and (ii) possibly higher loss due to conductor losses in the patch, dielectric losses in the substrate, and surface waves associated with the substrate.

**Conclusion:** Aperture-coupled patches allow relatively simple construction of waveguide-fed arrays for along-the-waveguide-axis polarisation. Incision into the broad wall is avoided. Thus, a scanning array with no grating lobes is easily fabricated. For weak-to-medium coupling factors, the fundamental propagating mode inside the waveguide is not perturbed, hence the desired scanning angle is easily controlled by the waveguide broad wall dimension.

**Acknowledgments:** This work was sponsored by Quadrant Engineering, Amherst, MA and NASA STTR contract NAS5-96045. The authors thank M. Goodberlet, of Quadrant Engineering, and Tan Huat Chio and J. Munro of the University of Massachusetts Antenna Laboratory for their help.

© IEE 1998

6 May 1998

Electronics Letters Online No: 19980915

W. Chang and D.H. Schaubert (Antenna Laboratory, Electrical and Computer Engineering Department, University of Massachusetts, Amherst, MA 01003, USA)

## References

- 1 STEVENSON, A.F.: 'Theory of slots in rectangular waveguides', *J. Appl. Phys.*, 1948, **19**, pp. 24-39
- 2 STERN, G.J., and ELLIOTT, R.S.: 'Resonant length of longitudinal slots and validity of circuit representation: Theory and experiment', *IEEE Trans. Antennas Propag.*, 1985, **AP-33**, pp. 1264-1271
- 3 JAN, G.G., SHU, P., and WU, R.B.: 'Moment method analysis of side-wall inclined slots in rectangular waveguides', *IEEE Trans. Antennas Propag.*, 1991, **AP-39**, pp. 68-73
- 4 AJOKA, J.S.: 'Two-mode waveguide slot array'. U.S. Patent 3503073, March 24, 1970
- 5 AJOKA, J.S., JOE, D.M., TANG, R., and NAM SAN WONG.: 'Arbitrarily polarized slot radiators in bifurcated waveguide arrays', *IEEE Trans. Antennas Propag.*, 1974, **AP-22**, pp. 180-184
- 6 POZAR, D.M.: 'Microstrip antenna aperture coupled to a microstrip line', *Electron. Lett.*, 1985, **21**, pp. 49-50

## Measured attenuation of coplanar waveguide on CMOS grade silicon substrates with polyimide interface layer

G.E. Ponchak and L.P.B. Katehi

The measured propagation constant of a coplanar waveguide on CMOS grade silicon with a polyimide interface layer is presented. It is shown that the transmission line can have an attenuation comparable to other transmission lines on Si substrates if the proper polyimide thickness is used.

**Introduction:** Recently, there has been increasing interest in the development of radio frequency integrated circuits (RFICs) based on Si manufacturing technology for low cost applications [1-3]. While the development of SiGe heterojunction bipolar transistors (HBTs) with a maximum frequency of oscillation,  $f_{max}$ , of 160GHz [4] has enabled Si-based circuits to be used in the millimetre-wave spectrum, it is the transmission lines and passive circuit elements that have limited the wider application of Si RFICs. Conventional RF transmission lines such as microstrip and coplanar waveguides (CPWs) placed on standard CMOS grade Si wafers with a resistivity of 1-20 $\Omega$ cm have an unacceptably high attenuation. To overcome this problem, two approaches have been used to fabricate Si RFICs.

The first employs Si wafers with a resistivity > 2500 $\Omega$ cm, which are usually called high resistivity silicon (HRS) substrates [1]. The advantage of using HRS is that transmission lines on it have a similar attenuation to transmission lines on GaAs [5]. Furthermore, equivalent circuit models developed for GaAs and other insulating substrates are applicable to circuits on HRS substrates. However, HRS wafers are more expensive and standard Si production processes may not be used.

An alternative solution is to use the polyimide layers that are frequently used in Si production processes to develop novel RF transmission lines [2, 3]. By placing a ground plane on the top side

of the Si and depositing a polyimide substrate over it, thin film microstrip (TFMS) lines may be fabricated. Since the electromagnetic fields are completely shielded from the lossy Si wafer, low attenuation is possible [5]. Furthermore, since via holes in the polyimide are easily fabricated using either wet or reactive ion etching, series and shunt circuit elements are easily integrated.

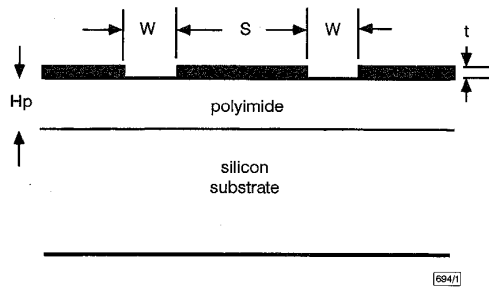


Fig. 1 Coplanar waveguide on low resistivity Si with polyimide interface layer

For microwave circuits, CPW is desirable because of the circuit layout advantages that result from having the ground planes and the signal strip on the same surface, but it is not practical to isolate CPW fields from the Si substrate with a metallic shield without exciting parasitic microstrip and parallel plate waveguide modes. This Letter experimentally investigates the use of polyimide layers on the surface of the Si to raise the CPW line above the lossy substrate, as shown in Fig. 1, and minimise the field interaction. The attenuation of this CPW structure is presented and compared to the attenuation of TFMS lines and CPW lines on HRS.

**Fabrication and test procedures:** Four sets of wafers with CPW lines are fabricated using Dupont WE1111 polyimide of thickness 6.35, 8.83, 14.59, and 20.15  $\mu\text{m}$ , 1.5  $\mu\text{m}$  of evaporated Au lines, and standard fabrication procedures. The lines are characterised using a vector network analyser and a microwave probe station with a quartz spacer between the wafer and the wafer chuck. The propagation characteristics are de-embedded through the thru-reflect-line (TRL) calibration routine implemented in the software program MULTICAL [6]. Each set of CPW lines consists of four delay lines, with the longest being 1cm, to cover the frequency range of 1–40GHz, a thru line, and a short circuit terminated line.

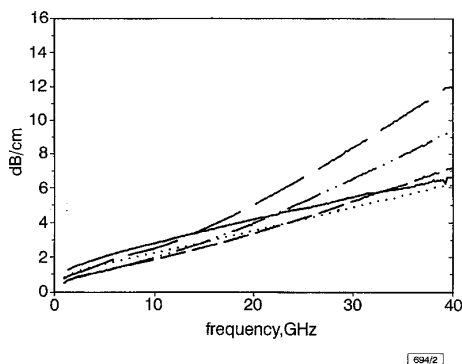


Fig. 2 Measured attenuation (dB/cm) of CPW lines on 14.59  $\mu\text{m}$  polyimide

- $S = 10, W = 4.5 \mu\text{m}$
- .....  $S = 20, W = 6 \mu\text{m}$
- $S = 30, W = 8 \mu\text{m}$
- · - ·  $S = 40, W = 10 \mu\text{m}$
- — —  $S = 50, W = 11 \mu\text{m}$

**Results:** The measured attenuation, in decibels/centimetre, of CPW lines on Si with a polyimide thickness of 14.59  $\mu\text{m}$  is shown in Fig. 2, where it is seen that the attenuation is dependent on the thickness of the polyimide and the strip and slot width. For small values of  $W/H_p$ , the attenuation is dominated by conductor loss, and the line has the characteristics of a CPW on a polyimide substrate; for wider slot widths, however, the attenuation increases dramatically. This is due to an increase in the frequency dependence of the attenuation from  $f^{0.5}$  to  $f^{1.5}$  as the ratio of  $W/H_p$  increases. There-

fore, unlike CPW on insulating substrates, the structures presented here have lower attenuation for CPW lines with narrower widths.

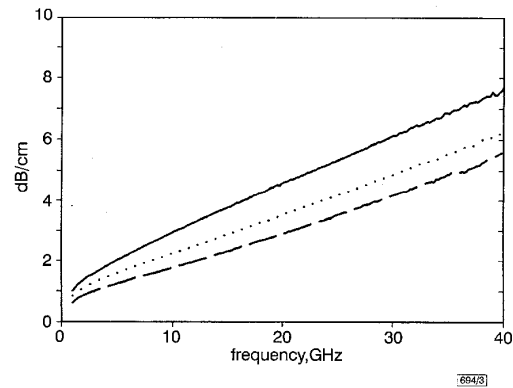


Fig. 3 Measured attenuation (dB/cm) of 50  $\Omega$  CPW lines against polyimide thickness

- $S = 10, W = 4.5, H_p = 8.83 \mu\text{m}$
- .....  $S = 20, W = 6, H_p = 14.59 \mu\text{m}$
- $S = 30, W = 8, H_p = 20.15 \mu\text{m}$

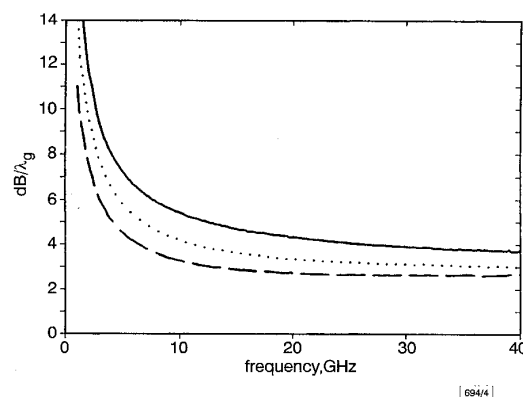


Fig. 4 Measured attenuation ( $\text{dB}/\lambda_g$ ) of 50  $\Omega$  CPW lines against polyimide thickness

- $S = 10, W = 4.5, H_p = 8.83 \mu\text{m}$
- .....  $S = 20, W = 6, H_p = 14.59 \mu\text{m}$
- $S = 30, W = 8, H_p = 20.15 \mu\text{m}$

Attenuation of 50  $\Omega$  CPW lines, in dB/cm, is shown in Fig. 3 against frequency and polyimide thickness, where it is seen that attenuation decreases as the polyimide thickness increases. This is also true for attenuation in  $\text{dB}/\lambda_g$  which is shown in Fig. 4. By comparing these results to other published results, the relative performance and usefulness of these transmission lines may be determined. CPW lines on low resistivity Si with polyimide have approximately the same attenuation in dB/cm at 40GHz, and lower attenuation below 30GHz (approximately 30% lower at 20GHz), compared to similarly sized CPW lines on HRS [5]. However, because the effective permittivity is lower due to the polyimide, the attenuation in  $\text{dB}/\lambda_g$  is approximately twice as large for the CPW lines presented here. Comparing CPW lines on polyimide with TFMS lines with a polyimide substrate [5] shows that both lines have similar attenuation per unit length below 10GHz, but TFMS has a lower attenuation at higher frequencies. The CPW on polyimide requires a polyimide thickness at least four times larger than the polyimide thickness of the TFMS lines to have a comparable attenuation of > 10GHz.

**Conclusions:** Coplanar waveguides fabricated on low resistivity silicon with a polyimide interface have been shown to have comparable attenuation per unit length to other transmission lines on Si substrates, if the polyimide is thick relative to the strip and slot width. Therefore, CPW lines on CMOS grade Si can be used for distribution networks and interconnects as an alternative to TFMS and CPW lines on high resistivity Si.

G.E. Ponchak (NASA Lewis Research Center, MS 54/5, 21000 Brookpark Road, Cleveland, OH 44135, USA)

L.P.B. Katehi (University of Michigan, 3240 EECS Building, Ann Arbor, MI 48109-2122, USA)

References

- 1 LUY, J.-F., STROHM, K.M., SASSE, H.-E., SCHUPPEN, A., BUECHLER, J., WOLLITZER, M., GRUHLE, A., SCHAFFLER, F., GUETTICH, U., and KLAABEN, A.: 'Si/SiGe MMIC's', *IEEE Trans. Microw. Theory Tech.*, 1995, **MTT-43**, (4), pp. 705-714
- 2 SUEMATSU, N., ONO, M., KUBO, S., IYAMA, Y., and ISHIDA, O.: 'L-band internally matched Si-MMIC front-end', *IEEE Trans. Microw. Theory Tech.*, 1996, **MTT-44**, (12), pp. 2375-2378
- 3 CASE, M., MAAS, S.A., LARSON, L., RENSCH, D., HARAME, D., and MEYERSON, B.: 'An X-band monolithic active mixer in SiGe HBT technology'. 1996 IEEE MTT-S Int. Microwave Symposium Dig., San Francisco, CA, 17-21 June 1996, pp. 655-658
- 4 GRUHLE, A., and SCHUPPEN, A.: 'Recent advances with SiGe heterojunction bipolar transistors', *Thin Solid Films*, 1997, **294**, pp. 246-249
- 5 PONCHAK, G.E., DOWNEY, A.N., and KATEHI, L.P.B.: 'High frequency interconnects on silicon substrates'. 1997 IEEE Radio Frequency Integrated Circuits Symp. Dig., Denver, CO, 8-11 June 1997, pp. 101-104
- 6 WILLIAMS, D.F., MARKS, R.B., and DAVIDSON, A.: 'Comparison of on-wafer calibrations'. 38th ARFTG Conf. Dig., San Diego, CA, 5-6 December 1991

Microwave switch based on S-N transition in high- $T_c$  superconducting film

A. Svishchev, I. Vendik, A. Deleniv, P. Petrov, A. Zaitsev and R. Wördenweber

An effective microwave switch using the transition from the superconducting state to the normal state (S-N transition) is presented. The main problem in designing an S-N switch arises from the low surface resistance of high- $T_c$  superconducting films in the N-state, which makes it difficult to obtain a low return loss. The authors have found a way to overcome this difficulty by including transformation circuits as an essential part of the S-N switch.

**Introduction:** It is well-known that the surface resistance of a superconducting film changes drastically under transport current. This effect has been used in microwave devices based on the S-N transition in high- $T_c$  superconducting (HTS) films: microwave switches, modulators, and phase shifters [1 - 5]. The S-N switching element is commonly used in the form of a relatively long narrow strip connected with a planar transmission line. The switching ability of the S-N switch can be evaluated by the commutation quality factor which is determined as [6]

$$K = \frac{R_N}{R_S} \quad (1)$$

where  $R_N$  and  $R_S$  are the surface resistances of the HTS film in the S- and N-states. The commutation quality is frequency and temperature dependent and, in practice, does not depend on the S-N element size and shape. The parameter  $K$  is very high for HTS films and, for  $T \leq 77K$  and  $F \leq 10GHz$ ,  $K \geq 10^4$ . This allows, in principle, the design of effective microwave switches. The insertion loss contributed by the S-N element in the S-state is negligibly small, and the isolation in the N-state can be remarkably high when using a long narrow strip. At the same time the return loss is limited by a small value of the surface resistance in the N-state (1-5Ω) and cannot be improved by increasing the length of the element. In none of [1 - 3, 5] is the problem of reflection coefficient in the N-state mentioned. Only in [4] it was discussed: the measured reflection coefficient  $S_{11} \approx -3dB$  against -20dB of insertion loss at  $f = 10GHz$  was observed. In the present paper we show how to obtain both high isolation and a large reflection coefficient using the S-N switching element.

**Theory:** We present the following relation between the scattering parameters of the switch in the N- and S- states:

$$|S_{21}^{(N)}| = |S_{11}^{(S)}| \quad (2)$$

Considering that the resistance of the switching element in two states is  $R^{(S)}$  and  $R^{(N)}$  and supposing that the element is connected in series with a transmission line with wave impedance  $Z_{01}$ , we find that eqn. 2 is satisfied when

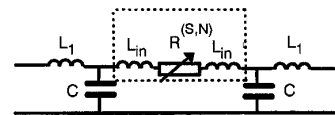
$$Z_{01} = 2\sqrt{R^{(S)} \cdot R^{(N)}} \quad (3)$$

The averaged resistance  $R_M = \sqrt{R^{(S)} \cdot R^{(N)}}$  is small (1-5 Ω). This means that transformation circuits should be included on both sides of the S-N element, hence matching  $2R_M$  with the wave impedance of the external transmission lines  $Z_0$ . In this case the condition of eqn. 2 is fulfilled as follows:

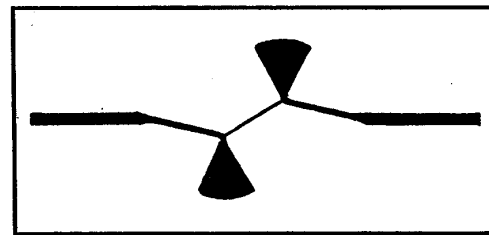
$$|S_{21}^{(N)}| = |S_{11}^{(S)}| = 1 - \frac{1}{\sqrt{K}} \quad (4)$$

The dual expressions are valid for the S-N switching element connected in shunt with a transmission line.

**Experimental details:** Fig. 1a presents the equivalent circuit of the S-N switch. The switching element is shown as the resistance  $R^{(S,N)}$  connected with two identical L-C matching circuits. Taking into account that the S-N switching element in the form of a narrow



a



b

Fig. 1 Equivalent circuit and layout of S-N switch

a Equivalent circuit  
 b Layout

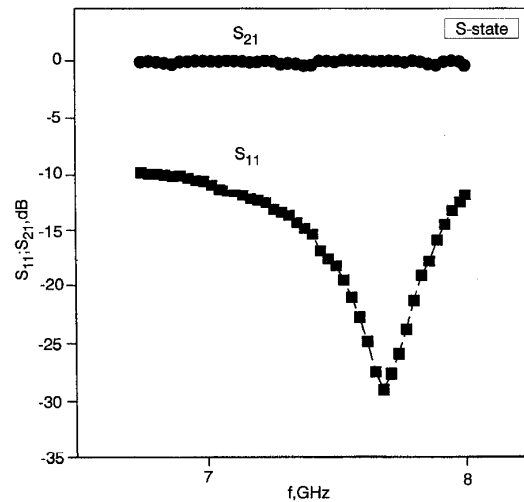


Fig. 2 Transmission  $S_{21}$  and reflection  $S_{11}$  coefficients of S-N switch in S-state (on-state)